

The Cut-off Wave Number for Weakly Nonlinear Wind Generated Surface Gravity Waves

Sergei A. Kitaigorodskii*

(Received: November 2014; Accepted: December 2014)

Abstract

In my recent papers (Kitaigorodskii, 2011a, 2011b, 2013a, 2014) the cut-off wavenumber k_g for weakly nonlinear waves in the inertial subrange was defined as

$$k_g^{-1} = \frac{\mathcal{E}_k}{\mathcal{E}_{t0}}, \quad (1)$$

where \mathcal{E}_k is the energy transfer rate (energy flux through the spectrum) and k_g^{-1} characterises the total width of the dissipation subrange. The formula (1) suggested by Kitaigorodskii (1983, 2013a) establish very important relationships between turbulent energy dissipation per unit mass, \mathcal{E}_{t0} , in turbulent patches that are formed by surfs, and the components of the energy balance in the equilibrium range of wind waves scales (Phillips et al., 2001). In this paper we present the results of the determination of k_g at different stages of the wave growth. This permits us to describe in some details the energy balance of wind waves and variability of air-sea interaction processes related to changes in the cut-off scale k_g .

Keywords: dissipation, turbulent kinetic energy, wind waves, dissipation scales, wave age

1 Introduction

The turbulent energy dissipation ε_t in the upper ocean is, according to Kitaigorodskii (1998, 2001)

$$\varepsilon_t = f(u_{*w}, z, K_0, z_{0d}), \quad (2)$$

where u_{*w} is the friction velocity in the upper ocean, z the depth, K_0 the turbulent viscosity defined by analogy with shear free turbulence where K_0 is independent of z (Long, 1978), and z_{0d} is the ocean surface roughness as seen from below, which according to the theory of Kitaigorodskii (2001) equals to

$$z_{0d} = 0.1 \frac{K_0}{u_{*w}} \text{ for } \frac{K_0}{\nu} \gg 1, \quad (3)$$

* Prof. S.A. Kitaigorodskii passed away 4th December 2014. He submitted this manuscript in November 2014. Editorial corrections were made by the co-editor Heidi Pettersson and the two reviewers before publication.

where ν is the kinematic molecular viscosity. Thus according to *Kitaigorodskii* (2001)

$$\varepsilon_t = \frac{u_{*w}^4}{K_0} F \left(\frac{u_{*w}z}{K_0} \right) \text{ for } z > z_{0d}. \quad (4)$$

The expression (4) is, strictly speaking, valid for neutral stratification. In the region of turbulent patches that form as a result of wind wave breaking $\left(\frac{u_{*w}z}{K_0} \sim O(1) \right)$ we can postulate that

$$\varepsilon_t = \varepsilon_{t0} = A_0 \frac{u_{*w}^4}{K_0} ; F = A_0 = const. \quad (5)$$

In (5) A_0 can depend on nondimensional characteristics of quasi-stationary conditions in the upper ocean such as nondimensional fetch or duration (wave age). The value of A_0 can also depend on the mechanisms of turbulent mixing chosen for determination of the eddy viscosity K_0 in (2) – (5). Only empirical determination of the variability of A_0 is available at the moment (*Kitaigorodskii*, 2011a, 2011b). However, as it will be shown in following sections, the variability of A_0 is one of the key factors in our understanding of interrelations between upper ocean turbulence and wind waves. According to (5) ε_{t0} may depend on both the velocity shear (through u_{*w}) and the turbulent energy flux directed deep from the center of the patch generated by the process of wave breaking (through K_0). Of course in formula (5) the effect of density stratification, when it is not negligible, is reflected in subsurface ocean layer. Also according to (3) and (4) we will not consider the structure of turbulence in the vicinity of the energy source, i.e. at $z \leq z_{0d}$.

The experimental data of *Terray et al.* (1996) and *Drennan et al.* (1996) has been used by *Kitaigorodskii* (2001) first of all to find the existence of a noticeable range of depths where (5) is valid together with the values of A_0 for different stages of wind wave growth (see Fig. 1). This Figure contains the information that was available about ε_{t0} in (2) at the moment of writing the paper. Of course, the parameterization of white-capping dissipation ε_{t0} in (5) by using *Long's* (1978) theory of shear free turbulence with an eddy viscosity K_0 constant in depth need some more detailed arguments. One of them is based on empirical knowledge that turbulent energy σ_t is proportional to the frequency of grid oscillations practically in all depths z . The other empirical feature of grid-generated turbulence is that turbulent energy decays with the distance from the grid as

$$\sigma_t \sim z^{-1}. \quad (6)$$

This lead to appearance of a constant (in depth) eddy viscosity K (*Long*, 1978):

$$K \sim \sigma_t l_t = const, \quad (7)$$

where $l_t \sim z$ is a scale of turbulence. Thus the shear free turbulence that can be generated by wave breaking can also have some features of the classical wall turbulence. How-

ever, and it was pointed out several times by *Kitaigorodskii* (2011a, 2011b), that asymptotic properties of such shear free turbulence generated by a source of energy with the size scale d (*Long*, 1978) of indefinitely small dimensions, for example the law

$$\varepsilon_t = \varphi(K_0) \sim \frac{K_0^3}{z^4} \tag{8}$$

are not supported by recent direct measurements of the subsurface turbulence (*Kitaigorodskii*, 2011b) in the ocean. Therefore we must assume either the influence of shear in (4) or closeness to the energy source described by the influence of z_{0d} .

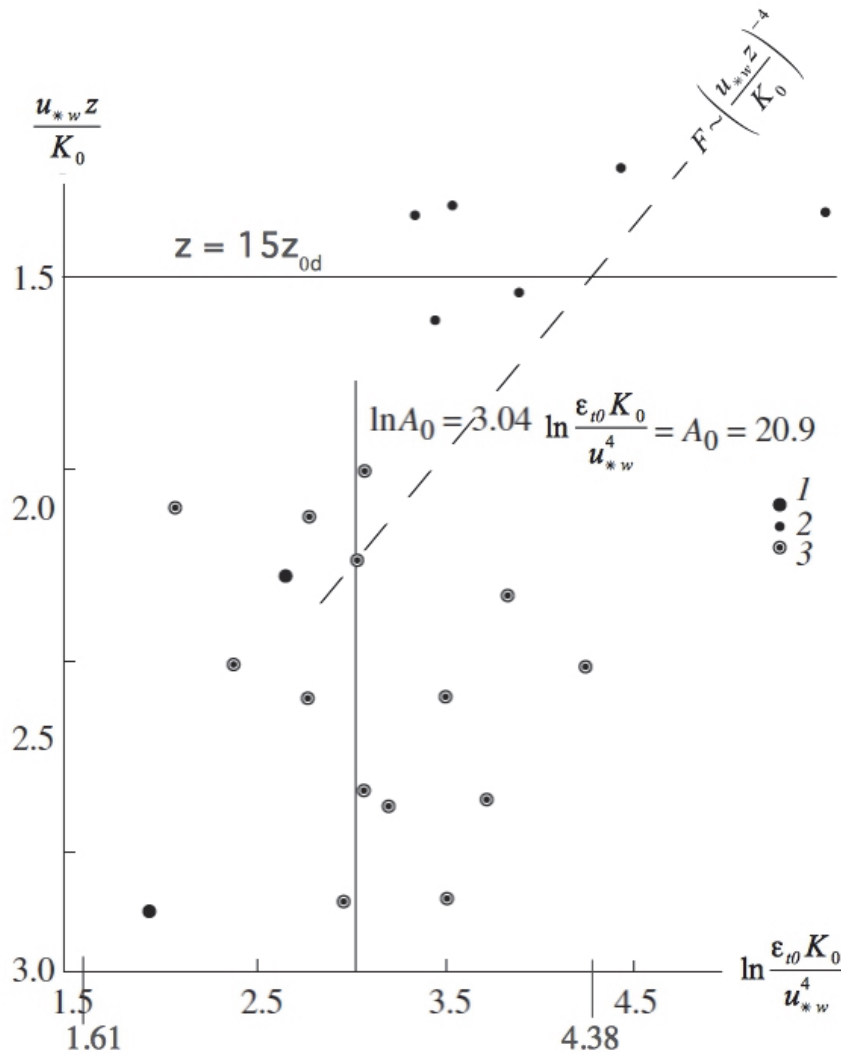


Fig. 1. Universal function $\varepsilon_{t0}K_0/u_{*w}^4 = F(u_{*w}z/K_0)$ (4) for the SWADE experiment data (Drennan et al. 1996). The average value of $A_0 = 20.9$ is shown as $\ln A_0 = 3.04$. Six points in the region $\varepsilon_t = \varepsilon_t(z)$ ($1.6 > u_{*w}z/K_0 > 1.2$ and the line corresponding to $z = 15z_{0d}$ are also shown. Modified from Figure 1 in *Kitaigorodskii* (2009, 2011a).

Remember that our energy source is just a continuous process of breaking (or overturning if you wish), which is present at the wavy sea surface. To characterize the

latter process with constant eddy viscosity we suggest that its scale estimate must be defined by at least two quantities – amplitude and frequency of breaking waves, i.e.

$$K_0 \approx a_{br}^2 \omega_{br} \quad (9)$$

where for estimates of a_{br} and ω_{br} the simplest way is to define them via spectral density of wave energy $S(\omega)$

$$a_{br} = \left[2 \int_{\omega_g}^{\infty} S(\omega) d\omega \right]^{1/2} \quad (10)$$

and ω_{br} can be identified with dissipation cut-off frequency ω_g

$$\omega_{br} = \omega_g ; k_{br}^{1/2} = \left(\frac{gk_g}{g} \right)^{1/2}. \quad (11)$$

Thus we come to *Kitaigorodskii's* (2001) suggestion to calculate K_0 through the relationship

$$K_0 = a_{br}^2 \omega_g = 2 \omega_g \int_{\omega_g}^{\infty} S(\omega) d\omega. \quad (12)$$

With

$$S(\omega) = \beta g^2 \omega^{-5} ; \omega \gg \omega_g ; \beta = 0.025 \quad (13)$$

the formula (12) will lead for nondimensional cut-off frequency $\frac{\omega_g U_a}{g} = 4.0$, where U_a is the wind speed, to

$$K_0 = 2 \cdot 10^{-4} \frac{U_a^3}{g} \quad (14)$$

and for $\frac{\omega_g U_a}{g} = 5.0$ to

$$K_0 = 1 \cdot 10^{-4} \frac{U_a^3}{g}. \quad (15)$$

Let us underline that the turbulent velocity scale $\sigma_t \sim a_{br} \omega_g$ based on a_{br} and ω_g is of the order of orbital velocities of small breaking gravitational surface waves, which we consider to be typical for whitecapping dissipation (*Phillips*, 1958), and thus have small values of Reynolds number $Re_t = \frac{\sigma_t a_{br}}{\nu} = \frac{a_{br}^2 \omega_g}{\nu}$ based on a_{br} . So the hypothesis of wave induced turbulence generated by exceeding the critical value of Re_t is not applicable for whitecapping turbulence. It is irrelevant even for larger waves¹ because of

¹ For larger wave amplitudes with Reynolds numbers $Re = \frac{a^2 \omega}{\nu}$, the effective turbulent viscosity strongly decays with depth as e^{-2kz} .

the domination of wind stress induced currents and shear turbulence in the upper ocean. That is why for a long time most of the efforts in studies of upper ocean turbulence in the presence of wind waves were concentrated on check-up of the classical relationship

$$\varepsilon_t = \frac{u_{*w}^3}{\kappa z} ; \kappa = 0.4. \quad (16)$$

It is not surprising that it was found that in data analysis the formula (16) works quite well (except in the very thin subsurface layer). Because of this the modelling of upper ocean turbulence considered for a long time that its structure is close to the classical wall layer turbulence.

Kitaigorodskii and Miropolskii (1968) took for the first time the effect of wave-generated turbulence into account in form of finite surface turbulent energy flux attributed to wind wave breaking. This idea was later used by *Graig* (1996) and *Graig and Banner* (1994) when they wanted to explain the enhanced level of turbulence in the upper ocean due to wind waves. This produces the need to use assumptions about z_{0d} – the roughness from below in the ocean surface layer. It was done unfortunately not in the form of *Kitaigorodskii-Long* theory (3). The comprehensive paper on modelling the upper ocean turbulence was published by *Benilov and Ly* (2002). The authors found that the shear free turbulence $K_0 = const$ is just one of the asymptotic regimes in the structure of the ocean turbulent boundary layer resulting in an existence of the inner sublayer with $K = const$ inside the whole turbulent boundary layer. Thus their work can be considered as a support for the justification of above used turbulence theory (2) – (15) in parameterization of the whitecapping dissipation.

2 The cut-off wave number for initial subrange in wind wave field in case of different energy balances in the equilibrium wave spectra

The formula (1), which we rewrite here as (*Kitaigorodskii*, 2013a)

$$\varepsilon_{t0} = \frac{\varepsilon_k}{k^{-1}} = g \varepsilon_k^{1/3} , \quad (17)$$

establishes a very important relationship between turbulent energy dissipation per unit mass ε_{t0} in turbulent patches that are formed by surfs and the components of the energy balance in the equilibrium range of wind wave spectrum. For example, if ε_k must characterize energy input from wind to waves, the estimate of ε_k in (17) can be done as in *Kitaigorodskii* (1983, 2013a):

$$\rho_w \varepsilon_k = \gamma \tau_a c_p, \quad (18)$$

where ρ_w is the water density, $\gamma \tau_a$ is the momentum flux to waves so that γ in (18) is a fraction of the total stress $\tau_a = \rho_a u_{*a}^2$ used by growing waves and c_p is the phase velocity of waves acquiring energy and momentum from the wind. Formula (18) can be rewritten as

$$\frac{\rho_w \varepsilon_k}{\rho_a u_{*a}^2} = \gamma c_p, \quad (19)$$

where γc_p can be defined as an effective phase speed $\bar{c} = \gamma c_p$ related to wind input (*Gemmrich et al.* 1994) for the equilibrium range of wind wave scales. In this range of scales (with phase speeds proportional to c_p and u_{*a}) the total wave dissipation according to *Phillips et al.* (2001) is

$$\rho_w \varepsilon_k = \rho_a u_{*a}^3 \hat{E} \ln \left(G \frac{c_p}{u_{*a}} \right) \quad (20)$$

where \hat{E} and G are numerical coefficients, which were taken in *Phillips et al.* (2001) as

$$\hat{E} = 2.5; \quad G = 0.5. \quad (21)$$

In the equilibrium range theory of *Phillips* (1985) the wind input (18) must be of the same order of magnitude as the dissipation in (20) and (21). This leads to

$$\gamma \frac{c_p}{u_{*a}} = 2.5 \ln \left(G \frac{c_p}{u_{*a}} \right). \quad (22)$$

For the range of observed $\frac{c_p}{u_{*a}} = 5 - 25$ (*Phillips et al.* 2001) the values of γ in (18) and (19) are in the range

$$\gamma \approx 0.4 - 0.16. \quad (23)$$

Such energy balance was accepted also in the classical paper of *Komen et al.* (1984) where the equilibrium state was considered as a result of competition of the wind input (18) with the wave dissipation (20) rather than a relaxation of wind sea to the inherent state due to the effect of resonant four wave nonlinear interactions. The latter view was advocated by *Badulin et al.* (2007) and *Zakharov and Badulin* (2011) who considered that the leading role of the nonlinear transfer in wind driven sea exists practically at all stages of wind wave growth. The corresponding formulations and comparison with data and numerical simulations can be found in the papers *Badulin et al.* (2007) and *Gagnaire-Renou et al.* (2011).

Kitaigorodskii (2013a) showed that the data analysis in the paper by *Gagnaire-Renou et al.* (2011) shows that the assumption of the dominance of nonlinear transfer in the inertial subrange implies that practically in all stages of wave development γ in (22) must be

$$\gamma \approx 10^{-2}, \quad (24)$$

which means that the region of energy input is strongly separated from the region of energy dissipation. This contradicts the conclusions of *Phillips et al.* (2001), but agrees with the conceptual picture of wind wave spectra proposed by the author as early as in 1961 (*Kitaigorodskii*, 2013a, 2013b). We will investigate below different cases of ener-

gy balance of the wind sea, including those when γ varies as in (22) – (24). We will emphasize that if (24) is really the case, i.e. wind input is concentrated at smaller phase speeds than c_p , this must enable the appearance of a region of inverse energy cascade, whose existence in *Zakharov and Badulin* (2011) was just postulated without any proofs (beside using the energy versus ω_p relations, which, as we mentioned before, cannot serve as a useful tool for testing different hypothesis about the energy balance for wind waves). Our calculations in terms of the variations of cut-off wave scales with the wave age give, for the first time, a reasonable qualitative explanation of the variations of the atmosphere-ocean interactions during the whole cycle of wind wave growth with the changes in the characteristics of the atmospheric turbulent boundary layers.

3 *The scaling for cut-off dissipation wave number and frequency for weakly nonlinear wind generated surface gravity waves*

To find the variability of the cut-off wavenumber k_g (formulas (1) and (17)) let us first consider the determination of the friction velocity u_{*w} in the water. We will use the commonly used expression based on the simplified form of the momentum balance

$$\tau_a - \gamma\tau_a = \tau_w = \rho_w u_{*w}^2, \quad (25)$$

which in (5) leads to

$$\varepsilon_{t0} = A_0 \frac{(1-\gamma)^2 \left(\frac{\rho_a}{\rho_w}\right)^2 u_{*a}^4}{K_0} \quad (26)$$

and to the following expression for k_g (see formulas (17) – (19))

$$k_g = \frac{u_{*a}}{K_0} \left\{ A_0 \frac{(1-\gamma)^2}{\gamma} \left(\frac{c_p}{u_{*a}} \right)^{-1} \frac{\rho_a}{\rho_w} \right\}. \quad (27)$$

The values of γ can be chosen with the *Phillips* (1985) suggestion to equalize energy input to dissipation, which leads in *Phillips et al.* (2001) to the range of values of 0.4 – 0.16 for γ (see (23)) when the observed range of values for c_p/u_{*a} is 0.2 – 0.04. Thus in (27) the corresponding values of $\frac{(1-\gamma)^2}{\gamma}$ are 0.9 and 4.4. This will give in (27) the following expression for k_g , now independent of $\frac{c_p}{u_{*a}}$ (for $\rho_a/\rho_w = 1.2 \cdot 10^{-3}$):

$$k_g = 0.21 \cdot A_0 \cdot 10^{-3} \frac{u_{*a}}{K_0}. \quad (28)$$

The estimates of A_0 in *Kitaigorodskii* (2011a, 2011b) gave $A_0 \approx 10^2$. So the final formula for k_g is

$$k_g = 0.21 \cdot 10^{-1} \frac{u_{*a}}{K_0}. \quad (29)$$

Two alternative estimates of K_0 can be done, the one based on classical shear turbulence theory with $K_0 \approx u_{*w} z_{0d}$ and the other based on Kitaigorodskii's theory on whitecapping dissipation with $K_0 \approx a_{br} \omega_g$. As the author has shown in several publications the direct measurements of turbulence below breaking wind waves favour his theory as a first approximation for description of the turbulent energy balance in the presence of strong whitecapping.

Thus $\frac{u_{*a}}{K_0}$ is a good possible scaling for k_g , since it permits to make a choice for K_0 that defines the scaling in terms of external parameters, in particular in terms of the wind speed. If we will use (9) for whitecapping K_0 with approximations (12) and (13), we have

$$K_0 = A_{00} \frac{U_a^3}{g} \quad (30)$$

where A_{00} depends on the choice of the value of nondimensional cut-off frequency $\tilde{\omega}_g = \frac{\omega_g U_a}{g}$ (Kitaigorodskii, 2013a) in (12) and (13). It follows that for the observed range of $\tilde{\omega}_g$, the values of A_{00} are in the range

$$A_{00} = (1 - 2) \cdot 10^{-4}. \quad (31)$$

The expression (27) can be rewritten with $A_{00} \approx 10^2$ (Kitaigorodskii, 2011a)

$$\frac{k_g U_a^2}{g} = \frac{0.21 \cdot 10^{-1} C_f^{1/2}}{A_{00}}, \quad (32)$$

where $C_f = \left(\frac{u_{*a}}{U_a}\right)^2$ is the drag coefficient for the sea surface, and A_{00} is given by (31). For $C_f = 1.3 \cdot 10^{-3}$ we have from (32)

$$\tilde{k}_g = \frac{k_g U_a^2}{g} = \frac{7.5}{(1-2)} ; \quad \tilde{\omega}_g = k_g^{1/2} = \frac{2.74}{(1-2)^{1/2}} = 2.7195. \quad (33)$$

This is just a crude estimate of $\tilde{\omega}_g$ which follows from (20) in this range of frequencies.

We will see how these values of \tilde{k}_g and $\tilde{\omega}_g$ agree with our previous estimates and observations. The above-mentioned formulas for cut-off wave number and frequency were received using well-known characteristics of interacting turbulent layers in the atmosphere (u_{*a}, U_a, z_0) and in the upper ocean (u_{*w}, K_0, z_{0d}). The other useful scaling for k_g can be based on its relation with z_{0d} – the roughness parameter from below. If for whitecapping turbulence z_{0d} is

$$z_{0d} = 0.1 \frac{K_0}{u_{*w}} \quad (34)$$

as was suggested by Kitaigorodskii (1994), then replacing K_0 in (27) we will get, instead of the scale $\frac{u_{*a}}{K_0}$, for k_g the following expression

$$k_g z_{0d} = \frac{A_0}{10} \left[\frac{(1-\gamma)^2}{\gamma} \left(\frac{c_p}{u_{*a}} \right)^{-1} \frac{\rho_a}{\rho_w} \frac{u_{*a}}{u_{*w}} \right]. \quad (35)$$

From (25) we have

$$\frac{u_{*a}}{u_{*w}} = \left(\frac{\rho_a}{\rho_w} \right)^{-1/2} (1-\gamma)^{-1/2} \quad (36)$$

and finally in (35)

$$k_g z_{0d} = \frac{A_0}{10} \left[\frac{(1-\gamma)^{3/2}}{\gamma} \left(\frac{c_p}{u_{*a}} \right)^{-1} \left(\frac{\rho_a}{\rho_w} \right)^{1/2} \right]. \quad (37)$$

For two values of $\frac{c_p}{u_{*a}}$ (5 and 25) and correspondingly two values of γ (0.4 and 0.16 in (23)) we have from (37):

$$\frac{(1-\gamma)^{3/2}}{\gamma} = 1.15 \text{ for } \gamma = 0.4, \text{ and } \frac{(1-\gamma)^{3/2}}{\gamma} = 4.8 \text{ for } \gamma = 0.16. \quad (38)$$

With $\left(\frac{\rho_a}{\rho_w} \right)^{1/2} = 0.034$ and the two values of $\frac{c_p}{u_{*a}}$, we finally get

$$k_g z_{0d} = A_0 (8 - 6.2) \cdot 10^{-4}. \quad (39)$$

If we accept as before the empirical value for $A_0 \approx 10^2$ then,

$$k_g z_{0d} \approx 0.08 - 0.062. \quad (40)$$

For the last value of $k_g z_{0d}$ in (40) we will have a rough estimate for the value of $\lambda_g = \frac{2\pi}{k_g}$:

$$\lambda_g = 10^2 z_{0d}, \quad (41)$$

which gives for example $\lambda_g = 1$ m when $z_{0d} = 1$ cm. This means that z_{0d} for the turbulence generated by whitecapping lies deep inside of the layer whose thickness is comparable to cut-off scales of wind waves.

To avoid any further speculations about proper scales for k_g and ω_g let us just use the *Phillips et al.* (2001) estimate of dissipation of the wind wave energy in our determination of the variability of dissipation scales in wind waves on the basis of turbulent energy dissipation in whitecapping subsurface turbulence (see (5) – (15)).

4 *Results of the calculation of the variability of the cut-off frequency for weakly nonlinear waves with wave age*

Let us start here with commonly used expression based on the simplified form of momentum balance (25), which leads to

$$u_{*w}^4 = \left(\frac{\rho_a}{\rho_w} \right)^2 u_{*a}^4 (1-\gamma)^2 \quad (42)$$

and thus to the expression (26) for ε_{t0} in (5). Now we can define k_g and ω_g – the cut-off wave number and frequency by equalizing the dissipation of wave energy in the dissipation subrange to the ε_{t0} defined in (26) – the dissipation of turbulent energy in the subsurface layer, where dissipation ε_t is presumed to be independent of the depth z (formulas (5) and (26)). The most natural way to do this is to accept the energy balance in the form given in (20), where the dissipation of wave energy that was measured directly for the first time by *Phillips et al.* (2001) can be taken according to formulas (20) and (21). That gives us the following expression for k_g :

$$k_g = \frac{A_0(1-\gamma)^2 \left(\frac{\rho_a}{\rho_w}\right) u_{*a}}{K_0 \hat{E}}. \quad (43)^*$$

This formula gives for the nondimensional wave number \tilde{k}_g and frequency $\tilde{\omega}_g$

$$\tilde{k}_g = \frac{k_g U_a^2}{g}; \quad \tilde{\omega}_g = \frac{\omega_g U_a}{g} = (\tilde{k}_g)^{1/2} \quad (44)$$

the following expression:

$$\tilde{k}_g = \tilde{\omega}_g^2 = \frac{C_f^{1/2} \frac{\rho_a}{\rho_w} (1-\gamma)^2 A_0}{\tilde{K}_0 \hat{E}}, \quad (45)$$

where

$$\tilde{K}_0 = \frac{K_0 g}{U_a^3} \quad \text{and} \quad C_f = \left(\frac{u_{*a}}{U_a}\right)^2 \quad (46)$$

are the nondimensional shear-free eddy viscosity \tilde{K}_0 and the drag coefficient for the sea surface C_f .

Our first calculations were made for a fixed value of the drag coefficient C_f . We, like many other air-sea interaction people thought that it could be characterized by a typical value in a narrow range $C_f = (1.1 - 1.3) \cdot 10^{-3}$. The recent estimates of C_f , especially for strong winds (hurricane type) indicate that its range can be much larger (*Bell et al.* 2012, *Kitaigorodskii*, 2014). Therefore in our calculations presented below we keep the observed range of C_f -values in the interval $(1 - 2.5) \cdot 10^{-3}$. This was done also because we want to demonstrate that the choice of the observed values of C_f does not influence our general physical conclusions about the wind wave growth proposed in this paper.

The other important unknown parameter in the balance of the energy and momentum in wind waves in our formulation described above is γ . Its values also can vary widely as was shown in Section 3. However, we are trying to find the existence of physically meaningful solutions, which can be independent of choice of the possible values of γ . We will discuss this question at the end of this section, but now let us first present some results of the calculations of \tilde{k}_g and $\tilde{\omega}_g$ based on our theory (43, 45). They will

* \hat{E} should be $\hat{E} \ln(G c_p / u_{*a})$, see Eqs. (20) and (22). Editor's remark.

show that the changes in the values of \tilde{k}_g and $\tilde{\omega}_g$ must be connected mainly with the changes in the stages of wind wave growth – so called inverse wave age characterized by the ratio of the wind speed U_a to the peak phase velocity c_p , $\frac{U_a}{c_p} = \frac{\omega_p U_a}{g} = \tilde{\omega}_p$.

To complete the calculations of \tilde{k}_g and $\tilde{\omega}_g$ we also must know the values of \tilde{K}_0 – the nondimensional turbulent viscosity for subsurface turbulence caused by whitecapping. These calculations, like was shown in *Kitaigorodskii* (2011a), require the knowledge of $\tilde{\omega}_g$, thus making the problem of determination of $\tilde{\omega}_g$ in (45) unclosed. However, as it was shown in *Kitaigorodskii* (2011a) such changes in K_0 can be easily estimated using our theory. For example the estimates in *Kitaigorodskii* (2011a, 2011b, 2014) show that for $\frac{\omega_g U_a}{g} = \tilde{\omega}_g = 5.0$, $\tilde{K}_0 = 1 \cdot 10^{-4}$ whereas for $\frac{\omega_g U_a}{g} = \tilde{\omega}_g = 4.0$, $\tilde{K}_0 = 2 \cdot 10^{-4}$. Therefore changes in K_0 are not too big for a reasonable range of values of $\tilde{\omega}_g$. Thus it will be useful to illustrate the range of the observed variations of $\tilde{\omega}_g$. The first attempt to do so was done in *Kitaigorodskii* (1998, 2004). Now we can find what is the range of theoretically derived values of \tilde{k}_g and $\tilde{\omega}_g$ in the framework of the theory in (43) and (45). For this we need to know the values of A_0 and γ in the relationship for \tilde{k}_g (45). We can parameterize A_0 according to the data from *Kitaigorodskii* (2011a). The corresponding formula can then be written as

$$A_0 = A_{01} \cdot 10^2 \tilde{\omega}_p^{-4} \quad (47)$$

and the range of A_{01} for values $\tilde{\omega}_g = 4.0 - 5.0$ is

$$A_{01} = 1 - 1.5. \quad (48)$$

An example of the empirical determination of A_0 based on the data from the SWADE experiment (*Drennan et al.* 1996) is presented in Fig. 1 (modified from *Kitaigorodskii* 2009 and 2011a). From Fig. 1 it follows that $A_0 = 20.9$ which according to (47) and (48) leads to the values $U_a/c_p = \tilde{\omega}_p = 1.47 - 1.63$. Thus the value of $A_0 = 20.9$ corresponds to rather mature waves, which were characteristic for the SWADE data, whereas formula (47) can describe variations of A_0 in other stages of the wave development. In Fig. 2 we present the results of our first calculations of the variation of $\tilde{\omega}_g$ with $\tilde{\omega}_p$, based on (17) and (19) and on a simplified form of the energy balance for a given value of the drag coefficient ($C_f = 1.3 \cdot 10^{-3}$) and for A_0 in (47) and (48).

The most important result of these calculations is the difference in the behaviour of $\tilde{\omega}_g$ with $\tilde{\omega}_p$ for different values of A_0 which was taken either constant ($A_0 = 20.9$) or according to the empirical findings (47, 48) in the relationship between A_0 and $\tilde{\omega}_p$ (*Kitaigorodskii*, 2011a). In the case of $A_0 = const$, a growth of $\tilde{\omega}_g$ with $\tilde{\omega}_p$ was observed. In our understanding this will contradict the traditional assumption of Kolmogorov's turbulence, where the inner dissipation scale diminishes with increasing energy supply. In weak wave turbulence based on the energy balance (1), the dissipation scale will increase with wave growth (and thus with the increase in energy supply to small

scales from larger scales). In other words, such difference in the behaviour of dissipation scale would mean that direct energy cascade typical for Kolmogorov's turbulence in the weak wave turbulence can lead to disappearance of the inertial range of scales opposite to Kolmogorov's turbulence where it increases with an increase in energy supply. This effect is due to the movement of white capping dissipation to longer (larger) wave components widening the dissipation subrange. According to the author this effect can be seen manifested in the increase of aerodynamic roughness of the sea surface in the presence of growing wind generated waves. That leads to the conclusion that only the direction of energy cascade (direct) is the factor that is common to the Kolmogorov's turbulence and to the weak wave turbulence applied to wind waves. The widening of the dissipation subrange in the field of wind generated waves can lead to the disappearance of the scales of inertial subrange and the direct energy cascade and any analogy of wind waves with the Kolmogorov's turbulence.

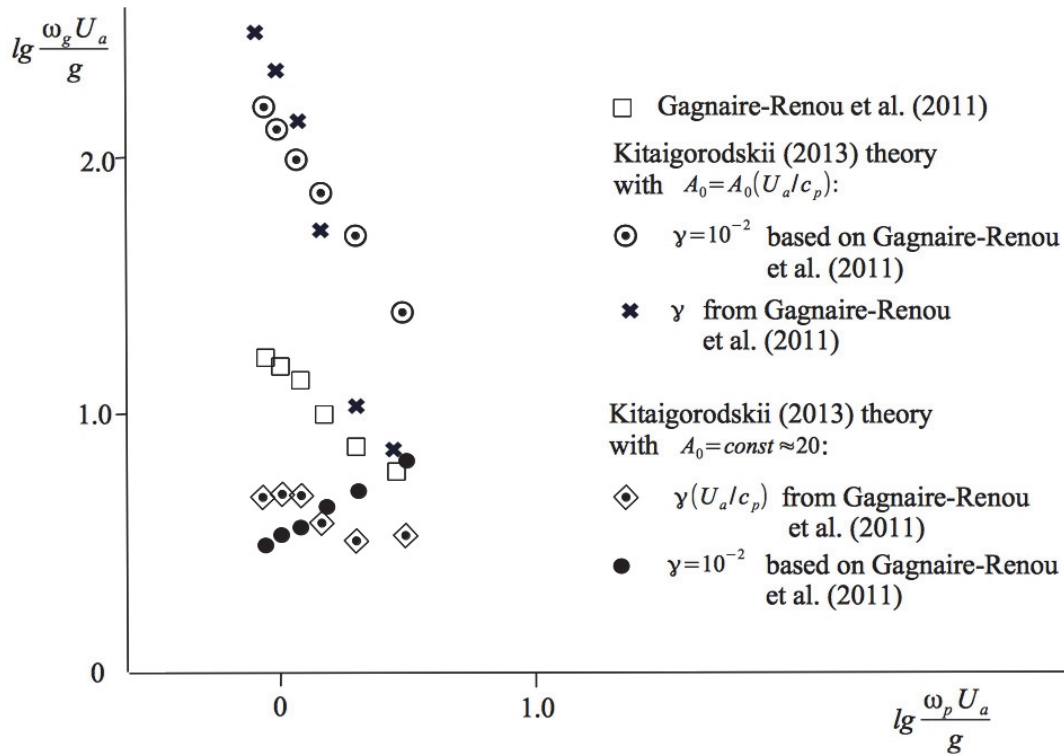


Fig. 2. The relationship between the nondimensional cut-off frequency $\tilde{\omega}_g = \omega_g U_a / g$ and nondimensional peak frequency $\tilde{\omega}_p = \omega_p U_a / g$ in different models (Kitaigorodskii, 2013a) based on the direct estimates of the dissipation of wave energy (Phillips *et al.* 2001) and the turbulent energy in the subsurface ocean layer (Kitaigorodskii, 2011a, 2011b).

The other important conclusion which can be drawn from the results of our calculations presented in Fig. 2, is that for a variable $A_0(\tilde{\omega}_p)$ and small values of γ , the width of the dissipation interval decreases as in traditional Kolmogorov's turbulence (when $\tilde{\omega}_g$ increases during downshift of $\tilde{\omega}_p$). This most likely corresponds to the inverse energy

cascade if the energy source remains in the region of short gravity waves. Thus the increase of $\tilde{\omega}_g$ with wave growth (downshift in $\tilde{\omega}_p$) can be attributed to appearance of the inverse energy cascade contrary to the traditional Kolmogorov's turbulence. This important aspect of Fig. 2 is illustrated in Fig. 3, which shows that the calculated (many prefer the word simulated) values of the cut-off frequency $\tilde{\omega}_g$ lie in the range of observed values $\tilde{\omega}_g$ versus $\tilde{\omega}_p$, as reported in *Kitaigorodskii* (1998, 2004). The observational evidence on the relationship between cut-off dissipation scale and stage of wave development does not permit to support only one possibility for the energy balance based on either direct or inverse energy cascades. The Figures we present here show that it is more likely that cascade regimes can change their direction during the wave growth. Fig. 2 illustrates this even more convincingly since it includes also the data from *Gagnaire-Renou et al.* (2011). It must be noted that only the latter data with $\gamma = \gamma(U_a/c_p)$ together with $A_0 = const = 20.9$ gives practically a constant value of $\tilde{\omega}_g$ ($\tilde{\omega}_g = 4 - 3.2$) which was found by *Kitaigorodskii* (2013a) as the most reliable average value of $\tilde{\omega}_g$. From Figs. 2 and 3 it follows that $\tilde{\omega}_g$ can be treated as a constant (or slightly varying with $\tilde{\omega}_p$) only for the case of $A_0 = const \approx 20.9$ (Fig. 1) and γ can also be considered as a constant in the simple form of energy balance (formulas (18) and (19)).

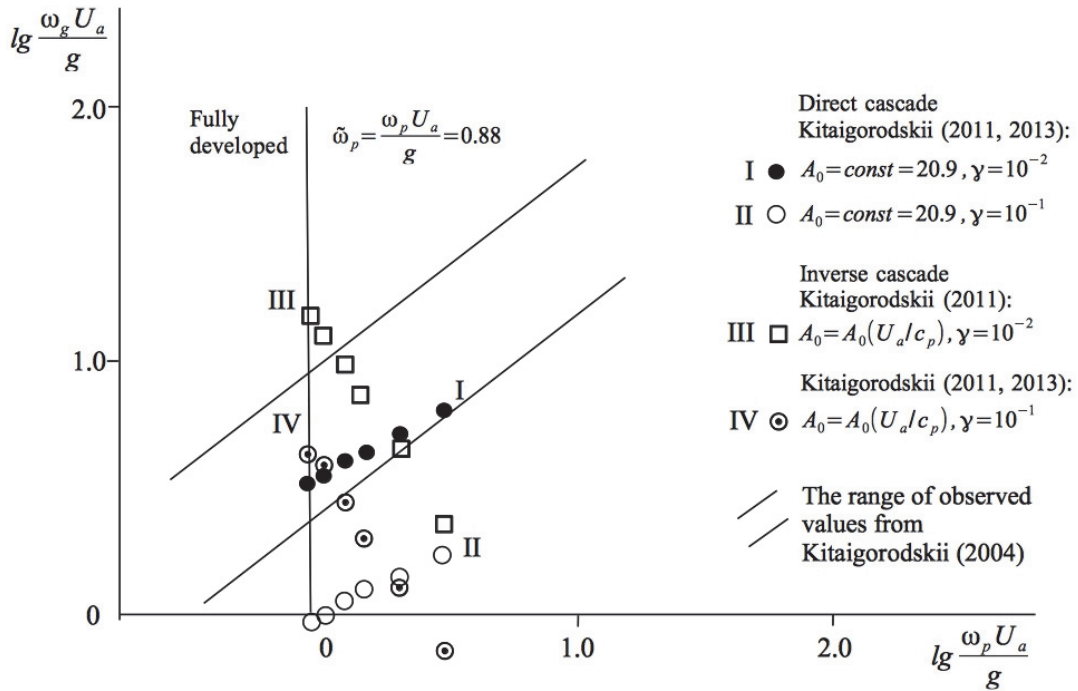


Fig. 3. Comparison of the calculated nondimensional cut-off frequency $\tilde{\omega}_g = \omega_g U_a / g$ in Fig. 2 with the observed data (*Kitaigorodskii*, 2004).

As we have mentioned above, the most natural way to use the existing data of the energy balance in wind waves in the form of (45) is when the dissipation of wave ener-

gy due to white capping is taken according to *Phillips et al.* (2001). Formulas (45) and (47) can give us the determination of \tilde{k}_g and $\tilde{\omega}_g$ where \hat{E} , the dissipation of wave energy, is from *Phillips et al.* (2001) and given by (20) and (21). Table 1 gives the values of \hat{E} in (20) and (21) for four values of the drag coefficient C_f . It shows that the main changes in the nondimensional wave dissipation \hat{E} during the wave growth occur when dissipation increases strongly from young to mature (or to fully developed) waves. However, we still do not know the behaviour of the drag coefficient C_f with the wave age.

Table 1. Different values of $\hat{E}(U_a/c_p)$ in (20) and (21) for four values of the drag coefficient C_f .*

U_a/c_p	$C_f = 1 \cdot 10^{-3}$	$C_f = 1.5 \cdot 10^{-3}$	$C_f = 2.0 \cdot 10^{-3}$	$C_f = 2.5 \cdot 10^{-3}$
0.5	8.61	8.11	7.74	7.49
0.88	7.19	6.69	6.5	6.07
1.0	6.89	6.39	6.02	5.77
2.0	5.17	4.67	4.3	4.05
5.0	2.89	2.39	2.02	1.77
10.0	1.14	0.64	0.27	0.02

The data presented in *Kitaigorodskii* (2014) shows that it can be rather complex – an increase at the first stages of the wave growth and a decrease at the last stages. Also the complete picture of the variation of C_f with the wind speed is not yet clear, largely because it must include badly known conditions in hurricanes with high wind speeds. The modelling of hurricanes gives a rather controversial picture. Therefore we have in Table 1 values of \hat{E} with different values of C_f from $(1 - 2.5) \cdot 10^{-3}$ (*Bell et al.* 2012). In Fig. 4 we present the result of the calculations with *Phillips et al.* (2001) values of \hat{E} for a fixed value for the drag coefficient $C_f = (1.0 - 1.3) \cdot 10^{-3}$. They have the similar character as the ones derived before without using the observed values of \hat{E} (*Phillips et al.* 2001). The two curves for $\tilde{\omega}_g$ versus $\tilde{\omega}_p$ based on \hat{E} are presented by dashed lines, the one for $A_0 = \text{const} = 20.9$, and the other for $A_0 = A_{01} \cdot 10^2 (U_a/c_p)^{-4}$. They are shown together with the previous calculations based on different values of γ .

However, we want to underline one new feature among the results presented in Fig. 4. If we choose the curves with the same value of γ , for example $\gamma = 10^{-2}$, and $A_0 = A_0(U_a/c_p)$, then the curves which we have associated with the "inverse cascade" and derived by using \hat{E} values from Table 1 (*Phillips et al.* 2001) cross the curves associated by us with the "direct cascade", which have the value $A_0 = \text{const} = 20$ and $\gamma = 10^{-2}$. They cross each other forming a triangle. The point of their crossing indicates the value of U_a/c_p ($\tilde{\omega}_p$) at which the direction of the energy cascades can change. The same is true for the two other curves in Fig. 4 for $\gamma = 10^{-1}$ and different A_0 ($A_0 = 20$ and $A_0 = A_0(U_a/c_p)$, formulas (47) and (48)). This general feature, as we will see later, is independent not only from our choice of the drag coefficient, but also, what is even more important, on the choice of γ , which characterize the momentum balance in wind wave field (42). Unfortunately the "triangle" on Fig. 4 by itself

* Converted from u_* scaling in *Phillips et al.* (2001). Editor's remark.

cannot provide an answer to the question of what type of cascade is dominating at the first and last stages of the wave growth. As we have shown above the constant value of $A_0 = 20.9$ (Fig. 1) must correspond to the mature waves rather close to the full development. That means that the relationship $A_0 = A_0(U_a/c_p)$ (47, 48) describes the increase of A_0 with the wave growth. This permit us to conclude that the part of the triangle associated with the calculation of $\tilde{\omega}_g$ using $A_0 = A_0(U_a/c_p)$, which we have associated with the inverse cascade, corresponds to the initial stages of wave growth (in Fig. 4 at $\log \frac{U_a}{c_p} \geq 0.24 - 0.36, \frac{U_a}{c_p} \geq 1.7 - 2.3$). It follows rather unexpectedly, at least for the author, that inverse energy cascade is dominating at the first stages of the wave growth, while the direct cascade is working from these stages of the wind wave growth up to the mature state. We can show later that such picture has a direct relation to the observed features of the variation in sea surface roughness with wave age. But now we will show that equation (43) with $\tilde{K}_0 = \text{constant} = (1 - 2) \cdot 10^{-4}$ can be written in the form

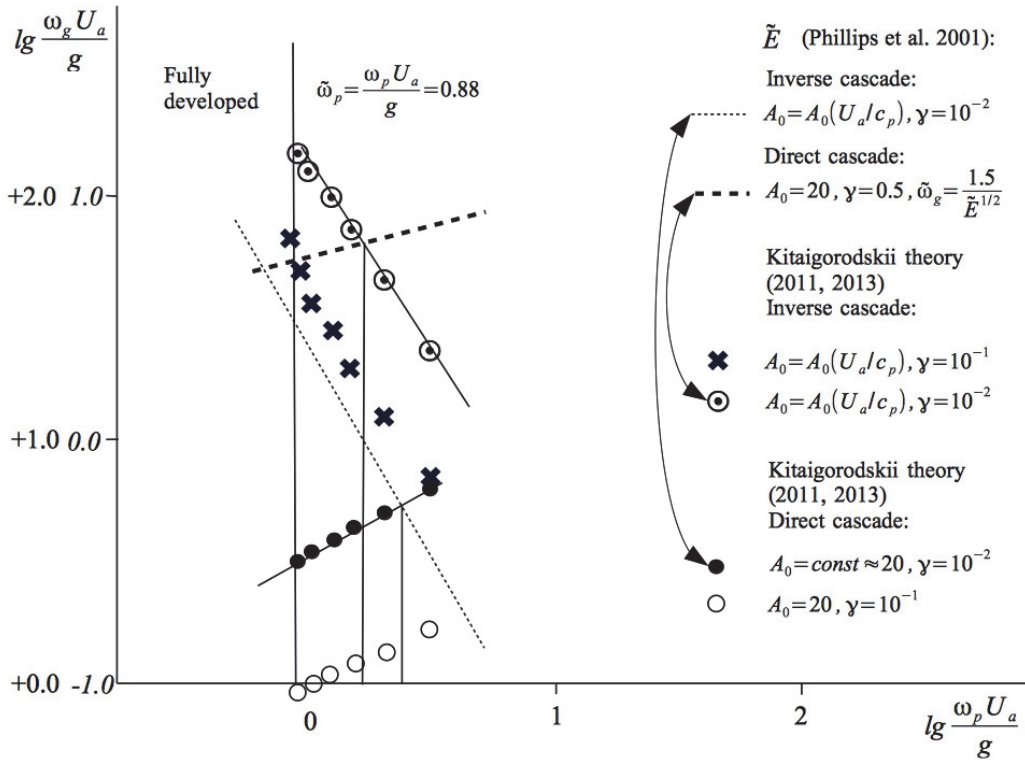


Fig. 4. Comparison of the nondimensional cut-off frequency $\tilde{\omega}_g = \omega_g U_a / g$ in Fig. 2 with the data calculated on the basis of Phillips et al. (2001) parameterization of the wave dissipation. The regions of potential existence of the inverse energy cascade at initial stages of wave growth (large $\tilde{\omega}_p = \omega_p U_a / g$) and the direct energy cascade at well developed waves are shown as two sides of a triangle based on different types of relationship between $\tilde{\omega}_g$ and $\tilde{\omega}_p$.**

** The y-scale [0 2] correspond to u_* scaling of \tilde{E} in Phillips et al. (2001). Editor's remark.

$$\frac{\tilde{\omega}_g^2}{(1-\gamma)^2} = \frac{10^3 C_f^{1/2} (\tilde{\omega}_p)^{-4}}{\hat{E}(\tilde{\omega}_p)}. \quad (49)$$

For four values of $C_f = (1.0, 1.5, 2.0, 2.5) \cdot 10^{-3}$ formula (49) can be rewritten as

$$\frac{\tilde{\omega}_g^2}{(1-\gamma)^2} = \frac{10^{3/2}(1.0-1.58)}{\hat{E}(\tilde{\omega}_p)\tilde{\omega}_p^4}. \quad (50)$$

Formula (49) is shown in Fig. 5 as the relationship between the cut-off frequency $\tilde{\omega}_g$ and $\tilde{\omega}_p$ for four values of the drag coefficient C_f ($\tilde{\omega}_g$ was normalised with $1 - \gamma$).

The dashed lines show the calculations that correspond to $A_{01} \approx 1.0 - 1.5$ and $\rho_a/\rho_w = 1.2 \cdot 10^{-3}$. As it was noted before, they can be associated with the inverse energy cascade when the width of the dissipation subrange diminished ($\tilde{\omega}_g$ moves to higher frequencies with wave growth) during the downshift of the peak frequency. The straight lines correspond to the $A_0 = const = 20$ and they are associated with direct energy cascade when the width of the dissipation subrange increases in the whitecapping process during the downshift of the peak frequency.

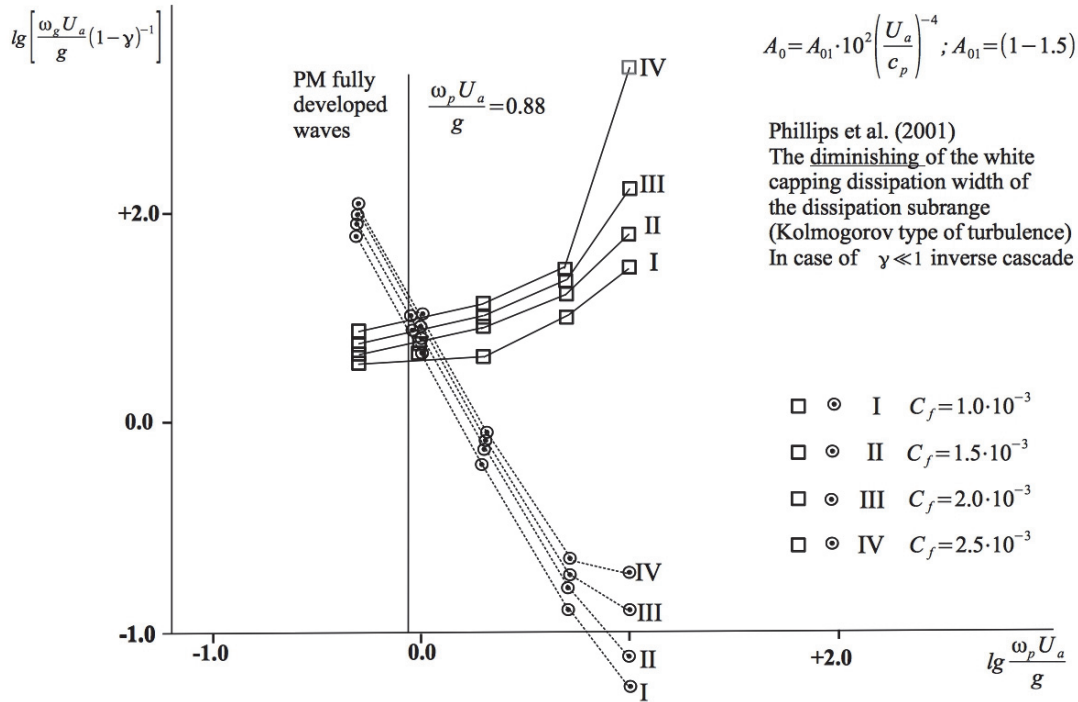


Fig. 5. The "Kitaigorodskii" triangles as in Fig. 4 calculated for four different values of the drag coefficient $C_f = 1.0, 1.5, 2.0, 2.5 \cdot 10^{-3}$ for normalized nondimensional cut-off frequency $\tilde{\omega}_g/1 - \gamma$ as a function of wave age $U_a/c_p = \omega_p U_a/g = \tilde{\omega}_p$.

As noted already, the crossings of these lines form a triangle whose sides corresponds to the initial stages of the wave growth and to the mature waves at the last stages of their development close to the full development. This period can be characterized as relaxation of wind wave spectra during the domination of the nonlinear effects in the

energy transfer in wind driven sea (*Zakharov and Badulin, 2011*). Thus the observed features in the behaviour of the cut-off dissipation wave frequency during the wind wave growth (Figs. 2–5) indicate the dominance of the inverse cascade in the nonlinear energy transfer in wind wave field at the initial stages of waves growth. Here it is worthwhile to quote a phrase from the interesting paper of *Zakharov and Badulin (2011)*: "One can suppose and then show numerically that the leadership of nonlinear transfer will be more definite at earlier stages of wave development when waves are lower but essentially steeper." Our Figures 2–5 confirm this conclusion, because the change to direct energy cascade happens when the growing waves are already well developed, as it was suggested in the scenario presented by the author in 1961. The dominance of the direct energy cascade in the growth of well-developed waves is not as well pronounced as the inverse cascade at early stages of wave growth. However, the presence of the change in the direction of the energy and momentum cascade in the wind wave field can serve to explain the observed variability of the sea surface roughness and drag coefficient including the regime of hurricane winds. A good approximation for the Charnock constant $m = gz_0/u_{*a}^2$ is related to the cut-off frequency $\tilde{\omega}_g$ according to the formula (15) in *Kitaigorodskii (2014)*, where $m \sim \tilde{\omega}_g^{-2}$. By taking into account the variation of $\tilde{\omega}_g$ with the inverse wave age $\tilde{\omega}_p$ as in Figs. 2–5, it is possible to explain the observed features in the variations of the Charnock constant m with the wave age shown in Figs. 1a and 1b in *Kitaigorodskii (2014)*.

References

- Badulin, S.I., A.V. Babanin, V.E. Zakharov and D. Resio, 2007. Weakly turbulent laws of wind-wave growth. *Journal of Fluid Mechanics*, **591**, 339–378.
- Bell, M.M., M.T. Montgomery and K.A. Emanuel, 2012. Air-sea enthalpy and momentum exchange at major hurricane wind speeds observed during CBLAST. *Journal of Atmospheric Sciences*, **69**, 3197–3222.
- Benilov, A.Yu and L.N. Ly, 2002. Modelling of surface waves breaking effects in the ocean upper layer. *Mathematical and Computer Modelling*, **35**, 191–213.
- Drennan, W.M., M.A. Donelan, E.A. Terray and K.B. Katsaros, 1996. Oceanic turbulence dissipation measurements in SWADE. *Journal of Physical Oceanography*, **26**, 808–815.
- Gagnaire-Renou, E., M. Benoit and S.I. Badulin, 2011. On weakly turbulent scaling of wind sea in simulations of fetch-limited growth. *Journal of Fluid Mechanics*, **669**, 178–213.
- Gemmrich, J.R. 2010. Strong turbulence in the wave crest region. *Journal of physical Oceanography*, **40**, 583–595.
- Gemmrich, J.R., T.D. Mudge and V.D. Polonichko, 1994. On the energy input from wind to surface waves. *Journal of Physical Oceanography*, **24**, 2413–2417.
- Graig, P.D. 1996. Velocity profiles and surface roughness under breaking waves. *Journal of Geophysical Research*, **101**, 1265–1277.

- Graig, P.D. and M.L. Banner, 1994. Modeling wave-enhanced turbulence in the ocean surface Layer. *Journal of Physical Oceanography*, **24**, 2546–2559.
- Kitaigorodskii, S.A. 1962. Applications of the theory of similarity to the analysis of wind generated wave motion as stochastic process. *Izvestia Academy of Science, USSR, Geophysics Series* **1**, 1961, 105–117. [English edition translated and published by the American Geophysical Union of theoretical Academy of Science, April 1962, 73–80].
- Kitaigorodskii, S.A. 1983. On the theory of the equilibrium range in the spectrum of wind-generated gravity waves. *Journal of Physical Oceanography*, **13**, 816–827.
- Kitaigorodskii S.A. 1994. A note on the influence of breaking wind waves on the aerodynamic roughness of the sea surface as seen from below. *Tellus*, **46A**, 681–685.
- Kitaigorodskii, S.A. 1998. Similarity theory as applied to the upper ocean turbulence. *Izvestia, Atmospheric and Oceanic Physics*, **34**(3), 430–434.
- Kitaigorodskii, S.A. 2001. On the influence of wind wave breaking on the structure of the subsurface oceanic turbulence. *Izvestia, Atmospheric and Oceanic Physics*, **37**(4), 566–576.
- Kitaigorodskii, S.A. 2009. Determining the influence of wind-wave breaking on the dissipation of the turbulent kinetic energy in the upper ocean and on the dependence of the turbulent kinetic energy on the stage of wind-wave development. *Izvestia, Atmospheric and Oceanic Physics*, **45**(3), 399–407.
- Kitaigorodskii, S.A. 2011a. The calculation of gas transfer between the ocean and atmosphere, (Eds. S. Komori, W. McGillis and R. Kurose): *Gas Transfer at water surfaces 2010, Kyoto University Press 2011*, 13–28.
- Kitaigorodskii, S.A. 2011b. The influence of wind wave breaking on the dissipation of the turbulent kinetic energy in the upper ocean and its dependance on the stage of wind wave development. (Eds. S. Komori, W. McGillis and R. Kurose) *Gas Transfer at water surfaces 2010, Kyoto University Press 2011*, 29–37.
- Kitaigorodskii, S.A. 2013a. Notes to the general similarity theory for wind generated nonlinear surface gravity waves. *Report series in Geophysics*, Department of Physics, University of Helsinki, Helsinki, Finland, **72**, 5–19.
- Kitaigorodskii, S.A. 2013b. Notes on the fundamentals of the modern methods in wind wave forecasting, *Report series in Geophysics*, Department of Physics, University of Helsinki, Helsinki, Finland, **72**, 20–39.
- Kitaigorodskii, S.A. 2014. On the Fundamentals in the Methods of Wind Wave Forecasting, *Geophysica*, **50**(1), 27–47.
- Kitaigorodskii, S.A. and Yu. Z. Miropolskii, 1968. Dissipation of turbulent energy in the surface layer of the ocean (English translation), *Izvestia Academy of Science, USSR, Atmosphere and Oceanic Physics*, **4**(6), 647–659.
- Komen G.J., S. Hasselmann and K. Hasselmann, 1984. On the existence of a fully developed wind-sea spectrum. *Journal of Physical Oceanography*, **14**, 1271–1285.
- Long, R.R. 1978. Theory of turbulence in a homogeneous fluid induced by an oscillating grid. *Physics of Fluids*, **21**, 1887–1888.

- Phillips, O.M. 1958. The equilibrium range in the spectrum of wind generated waves. *Journal of Fluid Mechanics*, **4**, 426–434.
- Phillips, O.M. 1985. Spectral and statistical properties of the equilibrium range in the spectrum of wind-generated gravity waves. *Journal of Fluid Mechanics*, **156**, 505–531.
- Phillips, O.M., F.L. Posner and J.P. Hansen, 2001. High range resolution radar measurements of the speed distribution of breaking events in wind-generated ocean waves: surface impulse and wave energy dissipation rates. *Journal of Physical Oceanography*, **31**, 450–460.
- Terray, E.A., M.A. Donelan, Y.C. Agrawal, W.M. Drennan, K.K. Kahma, A.J. Williams, P.A. Hwang and S.A. Kitaigorodskii, 1996. Estimates of kinetic energy dissipation by breaking waves. *Journal of Physical Oceanography*, **26**, 792–807.
- Zakharov, V.E. and S.I. Badulin, 2011. On energy balance in wind-driven sea, *Doklady Earth Sciences, oceanology*, **440**, 1440–1444.